Cell Metabolism
Article

Mineralocorticoid Receptor Phosphorylation Regulates Ligand Binding and Renal Response to Volume Depletion and Hyperkalemia

Shigeru Shibata,[1] Jesse Rinehart,[2] Junhui Zhang,[1] Gilbert Moeckel,[3] María Castañeda-Bueno,[5,6] Amy L. Stiegler,[4] Titus J. Boggon,[4] Gerardo Gamba,[5,6] and Richard P. Lifton[1,*]
[1]Department of Genetics and Howard Hughes Medical Institute
[2]Department of Cellular and Molecular Physiology and Systems Biology Institute
[3]Department of Pathology
[4]Department of Pharmacology
Yale University School of Medicine, New Haven, CT 06510, USA
[5]Molecular Physiology Unit, Instituto de Investigaciones Biomédicas, Universidad Nacional Autónoma de México, Tlalpan, 14000 Mexico City, Mexico
[6]Instituto Nacional de Ciencias Médicas y Nutrición Salvador Zubirán, Tlalpan, 14000 Mexico City, Mexico
*Correspondence: richard.lifton@yale.edu
http://dx.doi.org/10.1016/j.cmet.2013.10.005

SUMMARY

Nuclear receptors are transcription factors that regulate diverse cellular processes. In canonical activation, ligand availability is sufficient to produce receptor binding, entraining downstream signaling. The mineralocorticoid receptor (MR) is normally activated by aldosterone, which is produced in both volume depletion and hyperkalemia, states that require different homeostatic responses. We report phosphorylation at S843 in the MR ligand-binding domain that prevents ligand binding and activation. In kidney, $MR^{S843\text{-}P}$ is found exclusively in intercalated cells of the distal nephron. In volume depletion, angiotensin II and WNK4 signaling decrease $MR^{S843\text{-}P}$ levels, whereas hyperkalemia increases $MR^{S843\text{-}P}$. Dephosphorylation of $MR^{S843\text{-}P}$ results in aldosterone-dependent increases of the intercalated cell apical proton pump and Cl^-/HCO_3^- exchangers, increasing Cl^- reabsorption and promoting increased plasma volume while inhibiting K^+ secretion. These findings reveal a mechanism regulating nuclear hormone receptor activity and implicate selective MR activation in intercalated cells in the distinct adaptive responses to volume depletion and hyperkalemia.

INTRODUCTION

Nuclear receptors play key roles in signaling throughout the body, modifying transcription of target genes in response to ligand binding (Mangelsdorf et al., 1995). Steroid hormone receptors reside in the cytoplasm in the apo (unliganded) state, bound to proteins such as heat shock protein 90. Ligand binding induces release from these proteins, translocation to the nucleus, binding to specific DNA sequences, and recruitment of coactivators or corepressors, resulting in altered transcription of targets (McKenna and O'Malley, 2002; Pratt, 1997). Other members, such as the retinoic acid, thyroid hormone, and peroxisome proliferator-activated receptors, are bound to DNA with corepressors in the apo state and activated by ligand binding (Glass and Rosenfeld, 2000; McKenna and O'Malley, 2002). In these classical models of receptor activation, binding and activation are constitutive in the presence of ligand.

Posttranslational modifications of nuclear receptors can modify receptor activity. Phosphorylation can modulate interaction with coactivators (Rochette-Egly et al., 1997; Choi et al., 2010), prevent receptor dimerization and DNA binding (Chen et al., 1999), and promote ubiquitination, leading to either degradation (Lin et al., 2002) or stabilization (Yin et al., 2006). Phosphorylation of the amino terminus of PPARγ is suggested to reduce ligand binding (Shao et al., 1998); the mechanism of this effect is unknown. There have been no reports of posttranslational modification of the ligand binding domain (LBD) altering ligand binding.

The mineralocorticoid receptor (MR, encoded by *NR3C2*) is expressed in renal epithelia, smooth muscle, endothelium, cardiomyocytes, and hippocampal neurons (Gomez-Sanchez et al., 2006; Nguyen Dinh Cat et al., 2010). MR is activated by the steroid aldosterone and also by cortisol in cells that do not express the enzyme 11β-hydroxysteroid dehydrogenase type 2 (11βHSD2) (Arriza et al., 1987; Funder et al., 1988).

Aldosterone is produced by adrenal glomerulosa in two physiologic states. Intravascular volume depletion leads to activation of the renin-angiotensin system (RAS), increasing levels of angiotensin II (AII). AII signaling via the type 1 AII receptor (AGTR1), a G protein-coupled receptor, increases aldosterone production. Hyperkalemia (increased plasma K^+ levels) also increases aldosterone production by directly depolarizing glomerulosa cells (Spät and Hunyady, 2004).

MR is in epithelia of the distal nephron, comprising the distal convoluted tubule (DCT) and both principal cells and intercalated cells of the connecting tubule (CNT) and collecting duct (CD) (Ackermann et al., 2010). In volume depletion, MR signaling in principal cells increases Na^+ reabsorption via the epithelial Na^+ channel (ENaC) and Cl^- absorption via paracellular flux

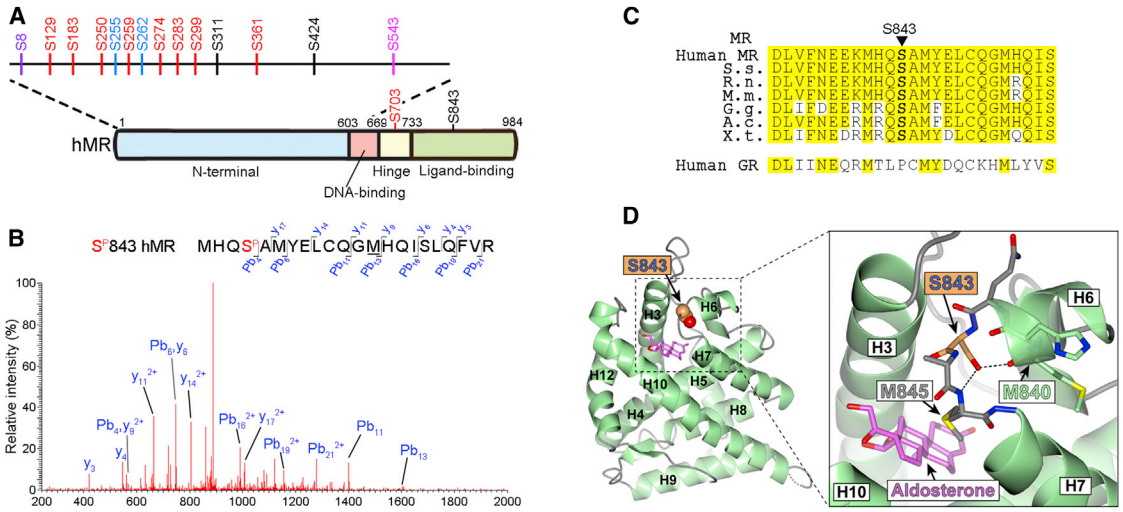

Figure 1. Phosphorylation Sites in Human MR

(A) Sites phosphorylated in MR in COS-7 cells are shown. Sites in motifs suggesting phosphorylation by proline-directed kinases (in red), glycogen synthase kinase-3 (blue), casein kinase II (purple), calmodulin kinase II (magenta), or no known kinase (black) are indicated.

(B) MS/MS spectrum of phosphopeptide containing S843-P is shown. The phosphorylated precursor ion, 911.73^{3+}, was selected and produced the fragment ion spectrum shown. Specific y and b fragment ions allowed assignment of phosphorylation at S843. Underline denotes oxidized methionine.

(C) Conservation of S843 among MR orthologs. S.s., *Saimiri sciureus*; R.n., *Rattus norvegicus*; M.m., *Mus musculus*; G.g., *Gallus gallus*; A.c., *Anolis carolinensis*; X.t., *Xenopus tropicalis*. Below is the sequence of human glucocorticoid receptor (GR); S843 is substituted to proline in all GRs.

(D) Location of S843 in the crystal structure of MR bound to aldosterone (PDB accession code 2AA2) (Bledsoe et al., 2005). Aldosterone (magenta), α helices (green) (H1-H11), loops (gray), and S843 (orange) are indicated. (Inset) H6-H7 loop showing hydrogen bonding of S843 side-chain hydroxyl with main-chain carbonyl and amino groups of M840 and M845, respectively. See also Figure S2.

(Beauwens et al., 1986). Signaling in DCT increases activity of the thiazide-sensitive Na-Cl cotransporter (NCC) (Reilly and Ellison, 2000). These activities maintain intravascular volume (see Figure S1A online). In hyperkalemia, MR-dependent reabsorption of Na^+ via ENaC provides a lumen-negative potential, driving renal K^+ secretion via the renal outer medullary K^+ (ROMK) channel (Figure S1B).

Consistent with these effects, gain-of-function mutations in MR lead to severe hypertension, often with hypokalemia (Geller et al., 2000). Conversely, loss-of-function mutations result in neonatal hypotension (Geller et al., 1998). Moreover, MR antagonists (MRAs) are effective antihypertensive drugs (Pitt et al., 2003).

In addition to these classical pathways, other mechanisms for electroneutral Na-Cl reabsorption in the distal nephron have been identified (Leviel et al., 2010; Wall and Pech, 2008). Combined activities of the apical H^+ ATPase of α-intercalated cells and the apical Cl^-/HCO_3^- exchanger (encoded by *Slc26a4*, *Pendrin*) of β-intercalated cells can couple ENaC-mediated Na^+ reabsorption and Cl^- reabsorption. Recently, an apical Na^+-dependent Cl^-/HCO_3^- exchanger (NDCBE) was implicated in electroneutral Na-Cl reabsorption via intercalated cells (Figure S1C) (Leviel et al., 2010). The roles of MR signaling in these processes are unknown.

Aldosterone production in both volume depletion and hyperkalemia poses a paradox: how does the kidney maximize Na-Cl reabsorption and minimize K^+ secretion in response to aldosterone in hypovolemia but maximize K^+ secretion in hyperkalemia? Explicit regulation of this balance is demonstrated by a Mendelian disease, pseudohypoaldosteronism type II (PHAII), in which aldosterone constitutively promotes renal Na-Cl reabsorption without K^+ secretion, producing hypertension and hyperkalemia. Mutations in kinases WNK1 and WNK4 (Wilson et al., 2001) cause PHAII via increased renal Na-Cl reabsorption (Wilson et al., 2003; Yang et al., 2003; Lalioti et al., 2006) and inhibition of K^+ secretion (Kahle et al., 2003). Similarly, mutations in ubiquitin ligase components CUL3 and KLHL3 (Boyden et al., 2012) cause PHAII by loss of degradation of WNKs (Shibata et al., 2013; Wakabayashi et al., 2013). WNK4 function is regulated by AII (San-Cristobal et al., 2009), suggesting AII signaling may play a role in the discrimination of these two states (Kahle et al., 2008). AII receptors are found on DCT, principal, and intercalated cells (Rothenberger et al., 2007).

We report identification of a phosphorylation site in the LBD of MR that regulates ligand binding and receptor activation, and we implicate this phosphorylation in producing distinct responses to aldosterone in volume depletion and hyperkalemia.

RESULTS

Identification of MR Phosphorylation Sites

FLAG-epitope-tagged human MR (Shibata et al., 2008) was expressed in COS-7 cells and purified by immunoprecipitation (IP) and SDS-PAGE. Samples were digested with trypsin, and phosphopeptides were purified using a TiO_2 matrix. Resulting peptides were identified by LC-MS/MS; phosphopeptides and specific sites of phosphorylation were assigned by the precise match of predicted and observed m/z ratios of precursor ions and their product fragment ions. In three independent mapping experiments, we reproducibly observed 16 phosphorylation sites in MR (Figures 1A and S2). Fourteen sites were in the

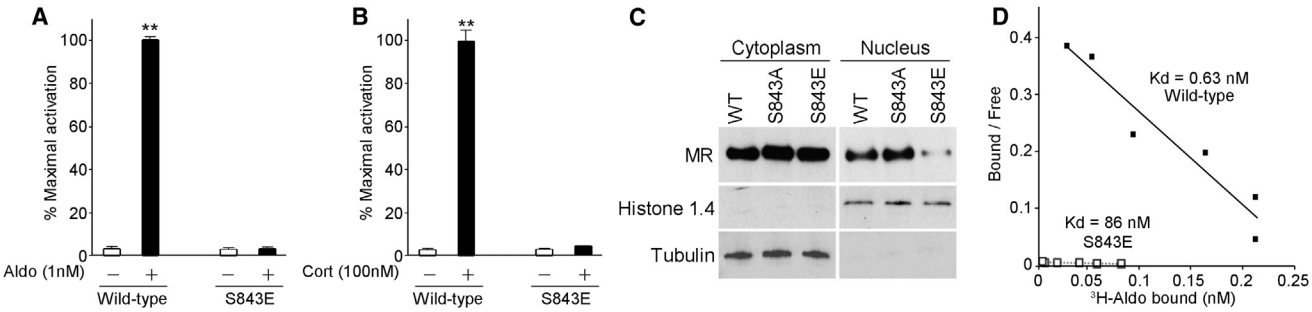

Figure 2. S843 Phosphorylation Inhibits MR Transactivation by Abrogating Ligand Binding

(A and B) Induction of luciferase under control of the MMTV promoter in COS-7 cells by wild-type (WT) MR and MR with the phosphomimetic S843E mutation in the presence or absence of 1 nM aldosterone (A) or 100 nM cortisol (B). Luciferase activity is expressed as percent of WT MR activity in the presence of ligand. Aldo, aldosterone; Cort, cortisol. Mean ± SEM is shown; n = 6 independent assays in each group; **p < 0.01.

(C) Localization of WT or mutant MR in nuclear and cytoplasmic fractions in the presence of 1 nM aldosterone. α-MR detects no signal without expression of MR. Unlike MR^{WT}, MR^{S843E} is almost exclusively cytoplasmic.

(D) Affinity of [^{3}H]aldosterone for MR. MR^{WT} and MR^{S843E} were expressed in COS-7 cells, and the binding affinity for [^{3}H]aldosterone and Scatchard analysis was performed. Each data point was analyzed in duplicate, and the mean value is shown. MR^{S843E} shows drastically reduced ligand binding. See also Figure S3.

amino-terminal domain, one each in the hinge region and LBD, and none in the DNA-binding domain. Sites identified included S129 and S250, previously reported to be phosphorylated in vitro by cyclin-dependent kinase 5 (Kino et al., 2010), and S361, phosphorylated by extracellular signal-related kinase (ERK) (Faresse et al., 2012); the remainder have not been reported. Nine amino-terminal and the hinge region phosphorylation sites harbored the minimal substrate motif (S-P) for phosphorylation by proline-directed kinases such as p38. Candidate kinases for other sites in the amino terminus included glycogen synthase kinase-3, casein kinase II, and calmodulin kinase II. The sole phosphorylation site in the ligand-binding domain, at serine 843 (S843) (Figures 1A and 1B), matched no known kinase motif.

Phosphorylation at S843 in the LBD was of particular interest. Serine at this position is conserved among orthologs from frogs to humans (Figure 1C). This site is implicated in the specificity of ligand binding. MR and glucocorticoid receptor (GR) evolved from a common MR-like ancestor. MR binds both mineralocorticoids (e.g., aldosterone) and glucocorticoids (e.g., cortisol), while GR selectively binds glucocorticoids. GR specificity derives from two substitutions in the LBD, one changing S843 in MR to proline (Ortlund et al., 2007). This suggested that phosphorylation of S843 might alter ligand binding and receptor activation. In the crystal structure of MR, S843 lies in the loop connecting H6 and H7 helixes of the LBD. In the ligand-bound state, the hydroxyl group of S843 forms hydrogen bonds with the carbonyl oxygen of M840 in helix H6 and the amino group of M845 (Figure 1D) (Bledsoe et al., 2005). Because these interactions stabilize the relationship between H6 and H7, phosphorylation of S843 might affect ligand binding and activation.

Phosphorylation at S843 Inactivates MR by Preventing Ligand Binding

We examined the effect of phosphorylation of S843 on the ability of MR to activate transcription of a luciferase reporter gene under control of the MR-responsive mouse mammary tumor virus (MMTV) promoter. Plasmids encoding wild-type (WT) MR (MR^{WT}) or MR with either a phosphomimetic glutamate substitution at position 843 (MR^{S843E}) or a nonphosphorylatable alanine substitution MR^{S843A} were expressed in COS-7 cells in the presence or absence of physiologic concentrations of aldosterone (1 nM) or cortisol (100 nM). Activation of MR^{WT} with either aldosterone or cortisol produced a >30-fold increase in luciferase activity (Figures 2A and 2B). MR^{S843A} showed similar activation (Figure S3A). In contrast, while expressed at levels indistinguishable from MR^{WT}, MR^{S843E} was not activated by either hormone (Figures 2A and 2B). No similar effects were observed at other MR phosphorylation sites tested with phosphomimetic or alanine substitutions (Figure S3A).

Apo-MR is normally cytoplasmic; aldosterone binding allows translocation to the nucleus (Pratt, 1997). We analyzed the subcellular distribution of WT and mutant MR by western blotting using α-MR antibodies in nuclear and cytoplasmic fractions. Both MR^{WT} and MR^{S843A} were abundant in the nucleus in the presence of 1 nM aldosterone (Figure 2C). In contrast, MR^{S843E} was virtually exclusively cytoplasmic. This conclusion was reinforced by IF microscopy of COS-7 cells expressing MR^{WT} or MR^{S843E} tagged with GFP (Figure S3B).

We evaluated receptor affinity for ^{3}H-labeled aldosterone for WT and mutant MR. The dissociation constant for aldosterone binding to MR^{WT} was 0.6 nM, consistent with prior studies (Arriza et al., 1987; Geller et al., 2000). In contrast, the dissociation constant for MR^{S843E} was 86 nM, a >130-fold increase (Figures 2D and S3C). This loss of ligand binding explains the loss of transcriptional transactivation and persistence of MR in the cytoplasm.

MR^{S843-P} Localizes to the Cytoplasm of Renal Intercalated Cells

We produced antibodies that specifically recognize MR phosphorylated at S843 (MR^{S843-P}) using an immunizing peptide that is identical in human and mouse. These antibodies selectively recognized synthetic MR peptide phosphorylated at S843, but not unphosphorylated peptide (Figure 3A). Western blotting of lysates from COS-7 cells expressing MR^{WT} identified a protein of the expected size (Figure 3B); this signal was abolished by alkaline phosphatase (Figure 3C) and absent in lysates

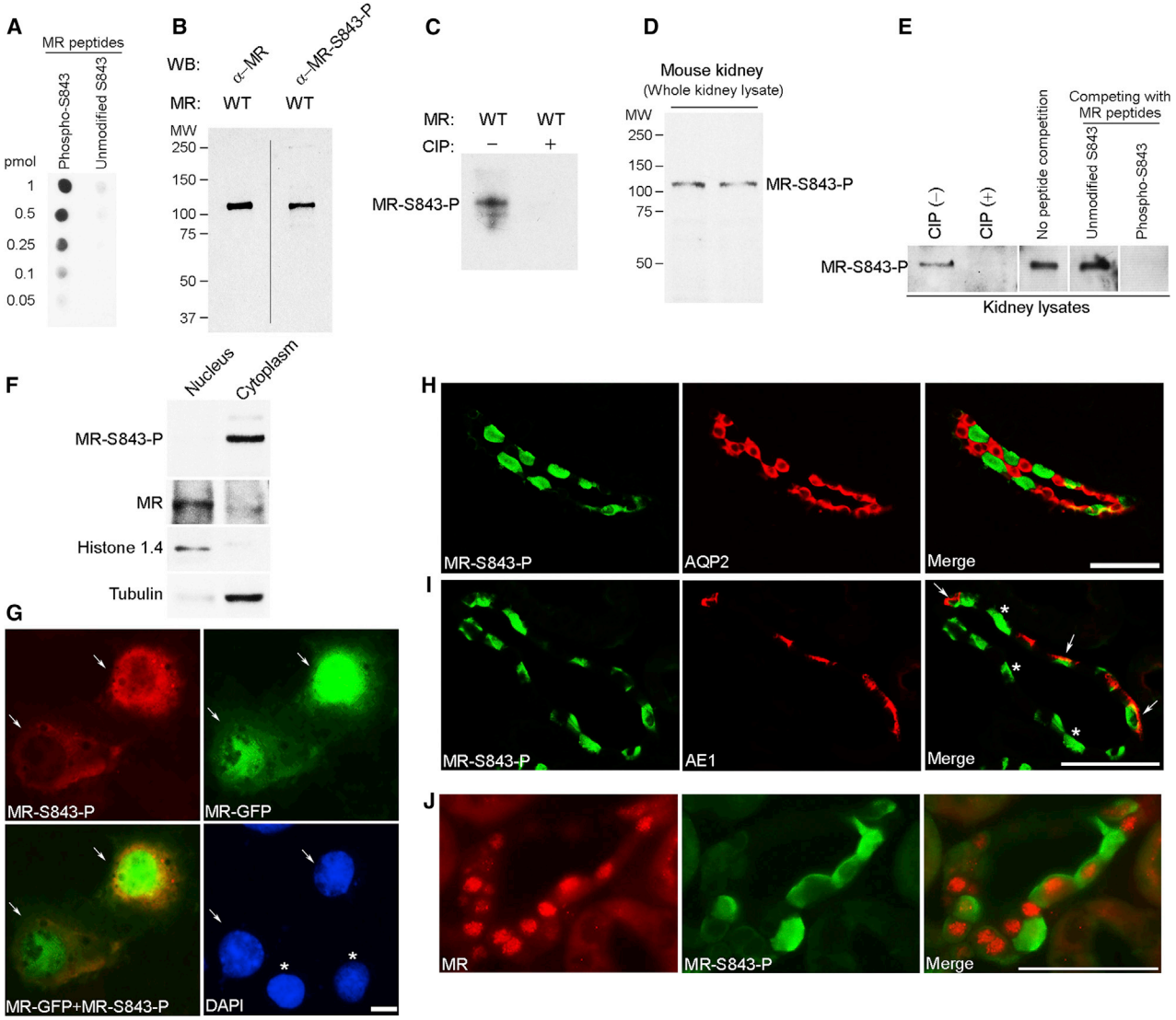

Figure 3. MR^{S843-P} Is Exclusively Cytoplasmic in Renal Intercalated Cells

(A) Antibodies specific for MR^{S843-P} (α-MR^{S843-P}) were incubated with phosphorylated and nonphosphorylated MR peptides spotted on a nitrocellulose membrane, followed by staining with peroxidase-conjugated donkey anti-rabbit antibody. The results demonstrate specificity for the phosphopeptide.

(B) Western blot of COS-7 cell lysates expressing human MR using antibodies to total MR or MR^{S843-P}. Samples were loaded in duplicate. α-MR^{S843-P} specifically recognizes a protein the size of MR.

(C) Phosphatase treatment eliminates α-MR^{S843-P} signal. FLAG-tagged human MR was purified, incubated with or without calf intestinal alkaline phosphatase (CIP), and analyzed by western blotting (see also Figure S4B).

(D) Expression of MR^{S843-P} in kidney. Total kidney lysates were prepared from mice fed normal chow and subjected to western blotting with α-MR^{S843-P}. The results from two mice are shown.

(E) Specificity of α-MR^{S843-P} in kidney lysates. Western blots of total kidney lysates from WT mice were stained with α-MR^{S843-P} without or with CIP treatment and then without peptide competition, with competition using the nonphosphorylated version of the immunizing MR peptide, then competition with the immunizing MR phosphopeptide. Phosphatase treatment or competition with immunizing phosphopeptide eliminates the antibody signal.

(F) Mouse kidney lysates were fractionated into nuclear and cytoplasmic fractions and stained with α-MR and α-MR^{S843-P} antibodies. Total MR is predominantly nuclear; MR^{S843-P} is confined to the cytoplasm.

(G) COS-7 cells expressing MR-GFP were stained with α-MR^{S843-P} antibody (red) and DAPI (blue) 1 hr after the addition of 1 nM aldosterone. Arrows indicate cells expressing MR-GFP, which were detected by fluorescence microscopy. MR-GFP was mainly nuclear, with less signal in the cytoplasm. In contrast, MR^{S843-P} was virtually exclusively cytoplasmic. No MR^{S843-P} signal was detected in cells that did not express MR-GFP (asterisks). Scale bar represents 10 μm.

(H) WT mouse kidney sections were stained for α-MR^{S843-P} (green) or AQP2 (a marker of principal cells in the CD, red). MR^{S843-P} is cytoplasmic and only seen in AQP2-negative cells (intercalated cells).

(I) Kidney sections were costained for MR^{S843-P} (green) and AE1 (red), which is expressed on the basolateral membrane of α-intercalated cells. MR^{S843-P} is found in AE1-positive cells (arrows) and also in some AE1-negative cells (asterisks, which are inferred to be β-intercalated cells; confirmed in Figure S4E).

(J) Kidney sections stained for α-MR (red) and α-MR^{S843-P} (green). Total MR is predominantly nuclear with half the cells (inferred to be intercalated cells) also showing cytoplasmic staining for MR^{S843-P}. Scale bars represent 50 μm in (H)–(J). See also Figure S4.

expressing no MR or MR^{S843A} (Figure S4A). These results establish the specificity of this antibody for MR^{S843-P}.

The subcellular distribution of MR with and without S843-P in COS-7 cells was evaluated by expressing MR-GFP (Shibata et al., 2008). In the presence of 1 nM aldosterone, total MR (identified by GFP fluorescence) was predominantly nuclear, with modest cytoplasmic staining. In contrast, MR^{S843-P} was confined to the cytoplasm (Figure 3G).

We surveyed tissues for MR^{S843-P} using this α-MR^{S843-P} antibody. By western blotting, we identified a protein of the appropriate size in kidney, but not in other tissues known to express MR (Figures 3D and S4C). This kidney signal is abolished by phosphatase treatment and by competition with the immunizing MR phosphopeptide, but not with unphosphorylated peptide (Figure 3E). Kidney homogenates fractionated into nuclear and cytoplasmic fractions showed that total MR was predominantly nuclear, while MR^{S843-P} was exclusively cytoplasmic (Figure 3F).

Immunofluorescence (IF) microscopy was used to determine the nephron segments and cell types that express MR^{S843-P}. Mouse kidneys were stained with α-MR^{S843-P} and either α-aquaporin 2 (AQP2), a marker of principal cells in the CNT and CD, or α-calbindin, an abundant protein in DCT. The results showed that MR^{S843-P} was confined to distal nephron segments that also stain for AQP2 (i.e., CNT and CD, Figure S4D). Surprisingly, in these distal nephron segments, MR^{S843-P} was found not in principal cells but instead exclusively in adjacent AQP2-negative epithelial cells (Figure 3H), which are presumptively α-intercalated and/or β-intercalated cells. This conclusion was confirmed by costaining for the Cl^-/HCO_3^- exchangers AE1, found in α-intercalated cells (Alper et al., 1989) (Figure 3I), and pendrin, found in the β-intercalated cells (Frische et al., 2003) (Figure S4E). MR^{S843-P} was found in both intercalated cell types. Moreover, MR^{S843-P} was confined to the cytoplasm in both (Figures 3H–3J). This localization was also found in human kidney (Figures S4F and S4G).

Volume Depletion and High Dietary Potassium Have Opposite Effects on MR^{S843-P}

We reasoned that there must be physiologic states that modulate S843 phosphorylation, converting the inactive phosphorylated form to a competent dephosphorylated form receptive to ligand. Because aldosterone secretion occurs with reduced intravascular volume or hyperkalemia, we examined levels of MR^{S843-P} when these parameters were changed. Intravascular volume was modulated by feeding mice high- or low-NaCl diets; we also compared littermates that were WT or homozygous deficient for the Na-Cl cotransporter NCC, encoded by *Slc12a3*, which results in volume depletion and activation of the RAS (Loffing et al., 2004). Low-NaCl diet resulted in a 50% reduction in MR^{S843-P} ($p = 0.001$, Figure 4A). Similarly, a 62% reduction was seen in $Slc12a3^{-/-}$ mice ($p = 0.007$, Figure 4B). In both cases, levels of total MR were unaltered. IF microscopy demonstrated that MR^{S843-P} is markedly reduced in both α- and β-intercalated cells in $Slc12a3^{-/-}$ (Figure 4C). Conversely, high-K^+ diet produced a marked increase in MR^{S843-P} (2.2-fold increase, $p = 0.0008$) (Figure 4D). Moreover, intercalated cell MR was predominantly cytoplasmic with high K^+ (Figure S5A, upper two panels) but was predominantly nuclear in $Slc12a3^{-/-}$ (Figure S5A, lower two panels). This is in contrast to the adjacent principal cells, in which MR is nuclear in both conditions (Figure S5A). These results suggest that intercalated cell MR is inhibited when increased K^+ secretion is required but is competent for activation in volume depletion.

Given the classical role of intercalated cells in acid/base physiology, we also tested whether MR^{S843-P} is modulated with changes in acid/base status. Acid loading was achieved by addition of NH_4Cl to the drinking water. This acid load induced the expected reduction in urinary pH, but western blot analysis revealed that MR^{S843-P} levels were not significantly altered (Figures S5B and S5C).

AII Signaling Produces Dephosphorylation of MR^{S843-P}

The modulation of MR^{S843-P} in opposite directions with volume depletion and potassium loading suggested that MR^{S843-P} might help orchestrate the different renal responses required in these two states. While both feature elevated aldosterone levels, only volume depletion produces increased AII. This observation, and the presence of AII receptors on intercalated cells (Rothenberger et al., 2007), suggested that AII signaling might contribute to dephosphorylation of MR^{S843-P}. We tested whether mice deficient for the AII type 1a receptor ($Agtr1a^{-/-}$) modulated MR^{S843-P} levels when changed from a high- to low-salt diet. $Agtr1a^{-/-}$ mice showed no reduction in MR^{S843-P} on low salt (Figure 4E), implicating AII signaling in dephosphorylation of MR^{S843-P} in volume depletion.

To directly test whether AII reduces levels of MR^{S843-P}, WT mice on high-NaCl diet received continuous infusion of AII (1 μg/kg/min, subcutaneously). This produced a 75% reduction in MR^{S843-P} with no change in total MR (Figures 4F and 4G). This effect was blocked by coadministration of losartan, an AII receptor blocker (ARB) (Figure 4F). IF microscopy confirmed that MR^{S843-P} was markedly reduced in both α- and β-intercalated cells (Figure 4H). These results demonstrate that AII signaling in the absence of volume depletion is sufficient to promote dephosphorylation of intercalated cell MR^{S843-P}.

Reduced MR^{S843-P} Increases Expression of Electrolyte Flux Mediators in Intercalated Cells

Dephosphorylation of MR^{S843-P} should produce receptor competence, allowing signaling in response to aldosterone. Likely MR targets in intercalated cells are mediators of electrolyte flux expressed in these cells. These include the multisubunit apical H^+ ATPase and the basolateral Cl^-/HCO_3^- exchanger AE1, both present in α-intercalated cells, and pendrin, an apical Cl^-/HCO_3^- exchanger in β-intercalated cells. We examined the expression of each of these by western blotting (the apical H^+ ATPase was assayed by levels of the B1 subunit, which is specific for the apical H^+ ATPase [Finberg et al., 2003]) (Figures 5 and S6). The results showed that levels of both the B1 subunit of the H^+ ATPase and pendrin were significantly increased with AII infusion and decreased with high dietary K^+ (Figure 5A). Similarly, both were elevated in $Slc12a3^{-/-}$ mice (Figure 5B), with increased apical membrane staining of the B1 subunit and pendrin (Figure S6D). These increases are dependent on AII signaling, as they are reversed by the selective AGTR1 inhibitor losartan (Figure 5C). Losartan also blocked the reduction in MR^{S843-P} levels in $Slc12a3^{-/-}$ (Figure S6F), consistent with AII regulating MR^{S843-P} dephosphorylation. MRA spironolactone,

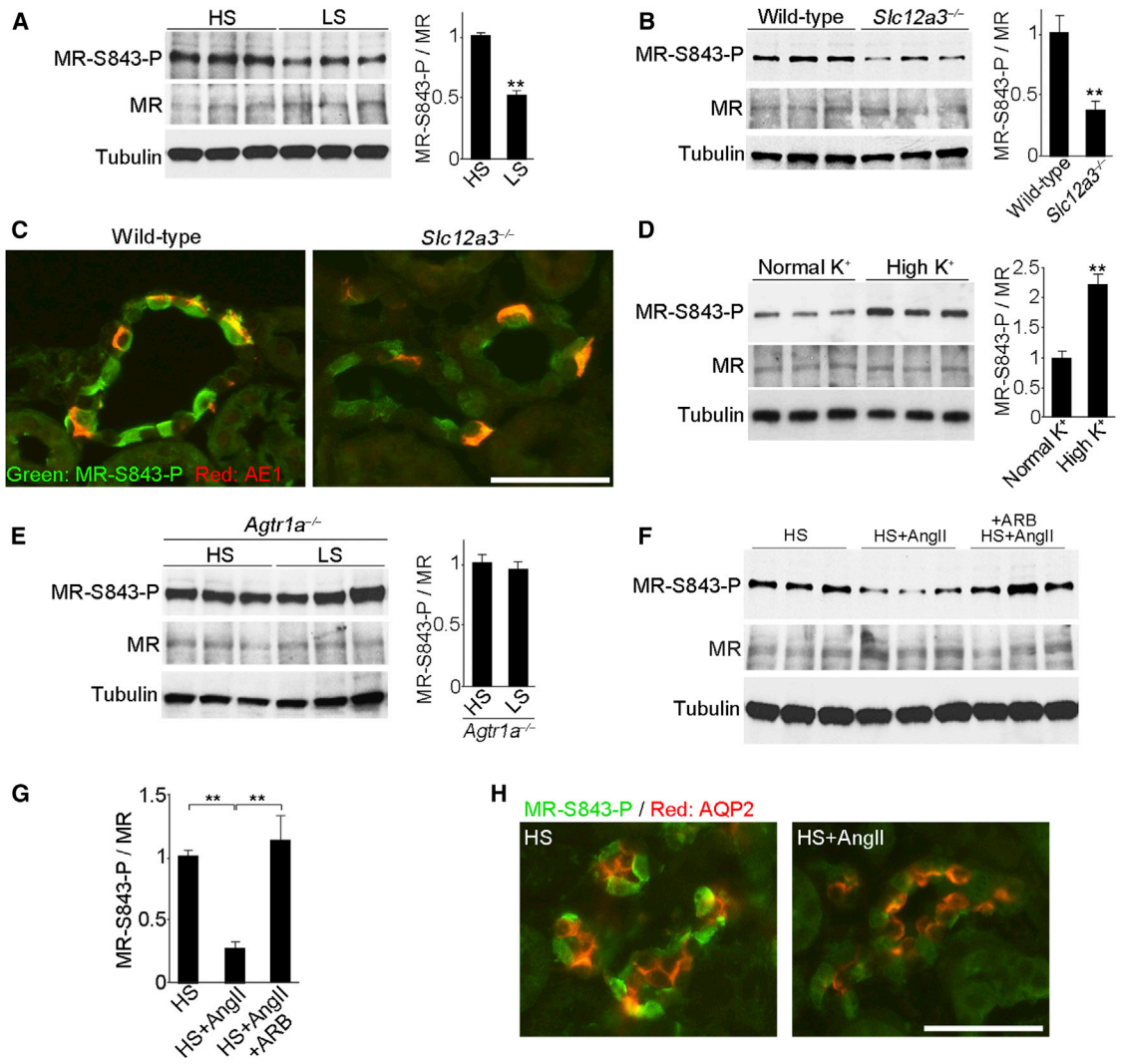

Figure 4. Changes in MR^{S843-P} with Volume Depletion, K^+ Loading, and AII Signaling

(A) MR^{S843-P} and total MR levels in kidneys of WT mice fed a high-salt (HS) or low-salt (LS) diet determined by western blot in biological replicates. Bar graphs show results of densitometric quantitation (n = 4 in each group).

(B) Levels of MR^{S843-P} in the kidneys of mice lacking NCC (*Slc12a3*$^{-/-}$) and WT littermates (n = 4). MR^{S843-P} is reduced in *Slc12a3*$^{-/-}$.

(C) Immunofluorescence microscopy of MR^{S843-P} (green) and AE1 (red) in kidneys of WT and *Slc12a3*$^{-/-}$ mice. MR^{S843-P} is markedly reduced in *Slc12a3*$^{-/-}$.

(D) MR^{S843-P} levels are increased in kidneys of WT mice eating a high-K^+ diet compared to normal diet (n = 4).

(E) MR^{S843-P} in kidneys of mice lacking type 1A AII receptor (*Agtr1a*$^{-/-}$) fed a high- or low-NaCl diet (n = 4). Low-salt diet fails to reduce levels of MR^{S843-P} in *Agtr1a*$^{-/-}$.

(F) AII infusion in WT mice fed high-NaCl diet reduces MR^{S843-P} levels; effect is prevented by an AII receptor blocker (ARB).

(G) Quantitation of MR^{S843-P} in the kidneys described in (F) (n = 3 or 4).

(H) Microscopy showing presence of MR^{S843-P} (green) and AQP2 (red) in kidneys of mice fed high-NaCl diet or high-NaCl diet with AII infusion. AII infusion reduces levels of MR^{S843-P}.

All error bars represent mean ± SEM; **p < 0.01. Scale bar represents 50 μm in (C) and (H). See also Figure S5.

however, did not prevent dephosphorylation in *Slc12a3*$^{-/-}$ (Figure S6F). Critically, if these effects of AII on intercalated cells require MR signaling, they should be prevented by MRA. This is indeed the case (Figure 5D). These findings establish that AII plus aldosterone signaling in intercalated cells together increase levels of the apical H^+ ATPase and pendrin, with increased dietary K^+ having the opposite effect, despite elevated aldosterone levels. These changes are likely adaptive in the physiologic responses to volume depletion and hyperkalemia (see below), as the combined activities of these electrolyte flux mediators are implicated in renal Na-Cl reabsorption (Pech et al., 2008; Soleimani et al., 2012).

In contrast, we found no significant effects of AII on AE1 expression (Figures S6B and S6C). Additionally, NDCBE appears to be regulated through an AII-dependent, MR-independent pathway, because AII increased NDCBE, but MRAs did not reverse these effects; moreover, hyperkalemia did not alter NDCBE levels (Figures S6B, S6C, and S6E).

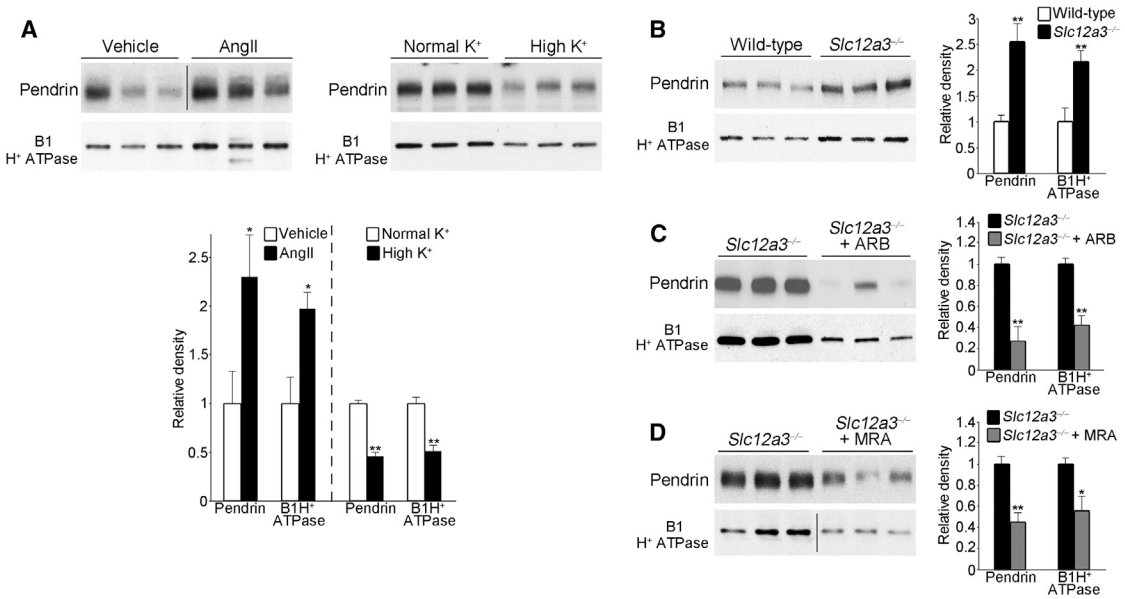

Figure 5. Modulation of MR^{S843-P} Alters Pendrin and B1 H$^+$ ATPase in Intercalated Cells

(A) Expression of pendrin and B1 H$^+$ ATPase in the membrane fraction of kidneys from indicated mice was analyzed by western blotting. Blots show biological replicates. Bar graphs show densitometric quantitation comparing levels of pendrin and B1 H$^+$ ATPase in indicated animals (n = 4 or 5 in each group).

(B) Membrane expression of pendrin and B1 H$^+$ ATPase in the kidneys obtained from WT and *Slc12a3*$^{-/-}$ (n = 4).

(C) Effects of ARB on pendrin and B1 H$^+$ ATPase membrane expression in the kidneys of *Slc12a3*$^{-/-}$ (n = 4).

(D) Effects of MR antagonist (MRA) spironolactone on pendrin and B1 H$^+$ ATPase membrane expression in the kidneys of *Slc12a3*$^{-/-}$ mice (n = 4).

Data are expressed as mean ± SEM; *p < 0.05, **p < 0.01. See also Figure S6.

WNK4 and PP1 Regulate Phosphorylation at MR^{S843}

The opposing effects of volume depletion and dietary K$^+$ on levels of MR^{S843-P}, and the effect of MR signaling in intercalated cells to modulate electroneutral Na-Cl reabsorption pathways (see below), suggest a potential role for the kinase WNK4 because of its known role in regulating the balance between Na-Cl reabsorption and K$^+$ secretion (Kahle et al., 2008; Wilson et al., 2001). Staining of mouse kidney with antibodies to WNK4 and markers of principal and intercalated cells demonstrated clear expression of WNK4 in intercalated cells (Figures 6A and S7A). We consequently investigated the effect of gain- and loss-of-function mutations in *WNK4* on levels of MR^{S843-P}. The TgWNK4^{Q562E} mouse (Lalioti et al., 2006) carries one extra copy of the *Wnk4* genomic locus harboring the gain-of-function Q562E mutation found in humans with hypertension and hyperkalemia (PHAII). Compared to WT littermates, these mice have a 62% lower levels of MR^{S843-P} (p = 0.017; Figure 6B). This is likely a primary effect of this mutation, since these mice have increased Na-Cl reabsorption, hypertension, and hyperkalemia (Lalioti et al., 2006), conditions that would otherwise be expected to increase MR^{S843-P} levels. Conversely, the *Wnk4* knockout mouse (Castañeda-Bueno et al., 2012) shows significantly increased levels of MR^{S843-P} (Figure S7B). These findings are consistent with WNK4 lying downstream of AII signaling in intercalated cells, as has been shown in DCT (San-Cristobal et al., 2009), and are consistent with WNK4^{Q562E} phenocopying AII signaling.

We evaluated the consequences of MR^{S843-P} dephosphorylation in TgWNK4^{Q562E} mice. At baseline, pendrin was slightly decreased and B1 H$^+$ ATPase was not different from WT littermates (Figure S7C), likely attributable in part to the acidosis seen in this model (Lalioti et al., 2006), as acidosis directly downregulates pendrin (Frische et al., 2003). We reasoned that the effect of MR^{S843-P} dephosphorylation may not be apparent in these mice, because, like their human counterparts, they do not have elevated serum aldosterone owing to suppressed plasma renin activity (Figure S7D). However, since MR is dephosphorylated, we expected that aldosterone should be capable of activating intercalated cell MR in this model. We thus infused aldosterone (50 μg/kg/day, s.c.) (Leopold et al., 2007) to TgWNK4^{Q562E} and WT littermates. Aldosterone infusion did not alter the levels of MR^{S843-P} (Figure S7E) but caused a marked increase in pendrin (2.7-fold increase, p < 0.0001) and B1 H$^+$ ATPase (2.1-fold increase, p < 0.0001) in TgWNK4^{Q562E} mice (Figures 6C and 6D). By contrast, aldosterone failed to upregulate pendrin and only marginally elevated B1 H$^+$ ATPase in WT littermates (Figures 6C and 6D). These results demonstrate that the MR-mediated increase in pendrin and B1 H$^+$ ATPase depends on both MR^{S843-P} dephosphorylation and aldosterone.

NDCBE was upregulated in TgWNK4^{Q562E} mice (Figure S7F), consistent with WNK4^{Q562E} phenocopying AII signaling (San-Cristobal et al., 2009). The levels of NDCBE were not altered by aldosterone infusion in WT or TgWNK4^{Q562E} mice (Figure S7G), confirming that NDCBE is regulated independently of MR signaling.

To identify the phosphatase responsible for dephosphorylation of MR^{S843-P}, we incubated purified FLAG-MR with protein phosphatases PP1, PP2A, and PP2B and assayed MR^{S843-P} by western blotting. Incubation with PP1 markedly reduced MR^{S843-P}, while other phosphatases did not (Figure S4B),

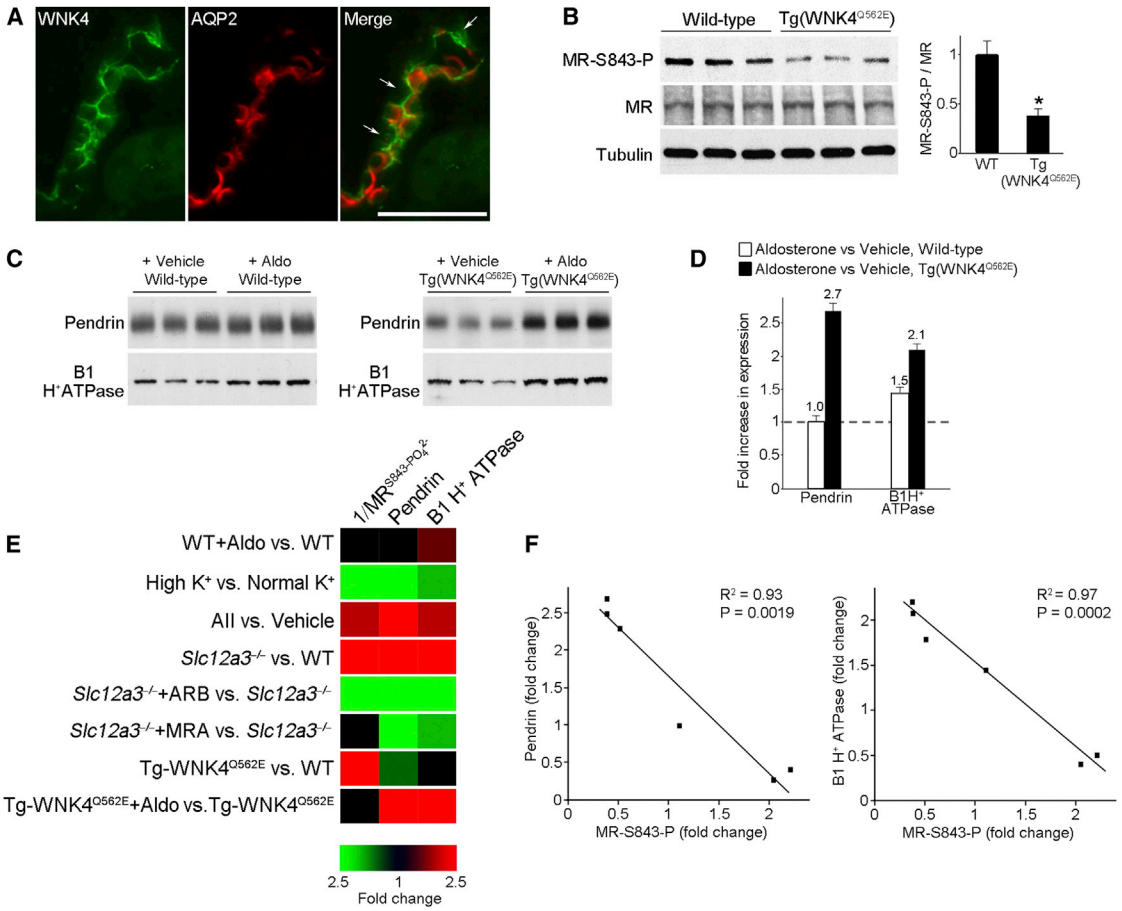

Figure 6. Role of WNK4 in Regulation of MR^{S843-P}

(A) Perfusion-fixed WT kidney sections were stained with α-WNK4 (green) or AQP2 (red). WNK4 is present in both AQP2-positive principal cells and in AQP2-negative intercalated cells (arrows; see also Figure S7A). Scale bar represents 50 μm.

(B) MR^{S843-P} levels in kidneys of $TgWNK4^{Q562E}$ mice carrying PHAII mutant WNK4 (Q562E) and WT mice. Blots show biological replicates. Bar graphs show results of quantitation (n = 4). Data are expressed as mean ± SEM; *p < 0.05.

(C and D) Effects of aldosterone infusion on the levels of pendrin and B1 H^+ ATPase in membrane fractions of kidneys from WT and $TgWNK4^{Q562E}$ mice. Bar graphs in (D) show the results quantitation in aldosterone-treated animals compared to controls (n = 6). Data are expressed as mean ± SEM.

(E) Parallel changes in levels of MR^{S843-P}, pendrin, and B1 H^+ ATPase in response to physiologic and genetic manipulations. Levels of MR^{S843-P} are inversely related to levels of B1 H^+ ATPase and pendrin; the increase in pendrin and B1 levels with dephosphorylated receptor is dependent upon aldosterone. Red indicates increased and green indicates decreased levels.

(F) Correlation of MR^{S843-P} and pendrin or B1 H^+ ATPase levels. Each data point compares the response of MR^{S843-P} and either pendrin (left) or B1 H^+ ATPase (right) in each physiologic or genetic manipulation described in (E) (comparisons of $Slc12a3^{-/-}$ + MRA to $Slc12a3^{-/-}$, and of Tg-$WNK4^{Q562E}$ to WT, in which aldosterone levels are not increased, are not included). For MR^{S843-P} levels in Tg-$WNK4^{Q562E}$ + aldosterone group, levels in WT mice are used as reference. See also Figure S7.

consistent with recent findings showing an interaction of WNK4 and PP1 (Lin et al., 2012).

DISCUSSION

We identified a phosphorylation site in the LBD of MR that renders the receptor incapable of ligand binding and activation; dephosphorylation results in aldosterone-dependent increases in proteins mediating intercalated cell electrolyte flux.

Across all experiments, the quantitative changes in MR^{S843-P} are highly correlated with changes in pendrin and B1 H^+ ATPase (Figures 6E and 6F). Demonstration that increases in pendrin and B1 H^+ ATPase require MR signaling provides strong evidence of a causal relationship.

MR^{S843-P} was found exclusively in renal intercalated cells, and its levels are modulated in opposite directions by the physiologic stimuli for aldosterone secretion, volume depletion, and hyperkalemia. Dephosphorylation in volume depletion is dependent on AII signaling and a downstream kinase, WNK4. Dephosphorylation restores MR competence and aldosterone-dependent increases of intercalated cell proteins that are adaptive to volume depletion (Figure 7). Increased apical H^+ ATPase and Cl^-/HCO_3^- exchange activity increases net Cl^- reabsorption, which in conjunction with aldosterone-induced Na^+ reabsorption by ENaC increases electroneutral Na-Cl reabsorption (Figure 7D) (Wall and Pech, 2008). In contrast, hyperkalemia increases phosphorylation of MR^{S843}, reducing levels of these proteins; in this setting, the lumen-negative potential from ENaC activity drives

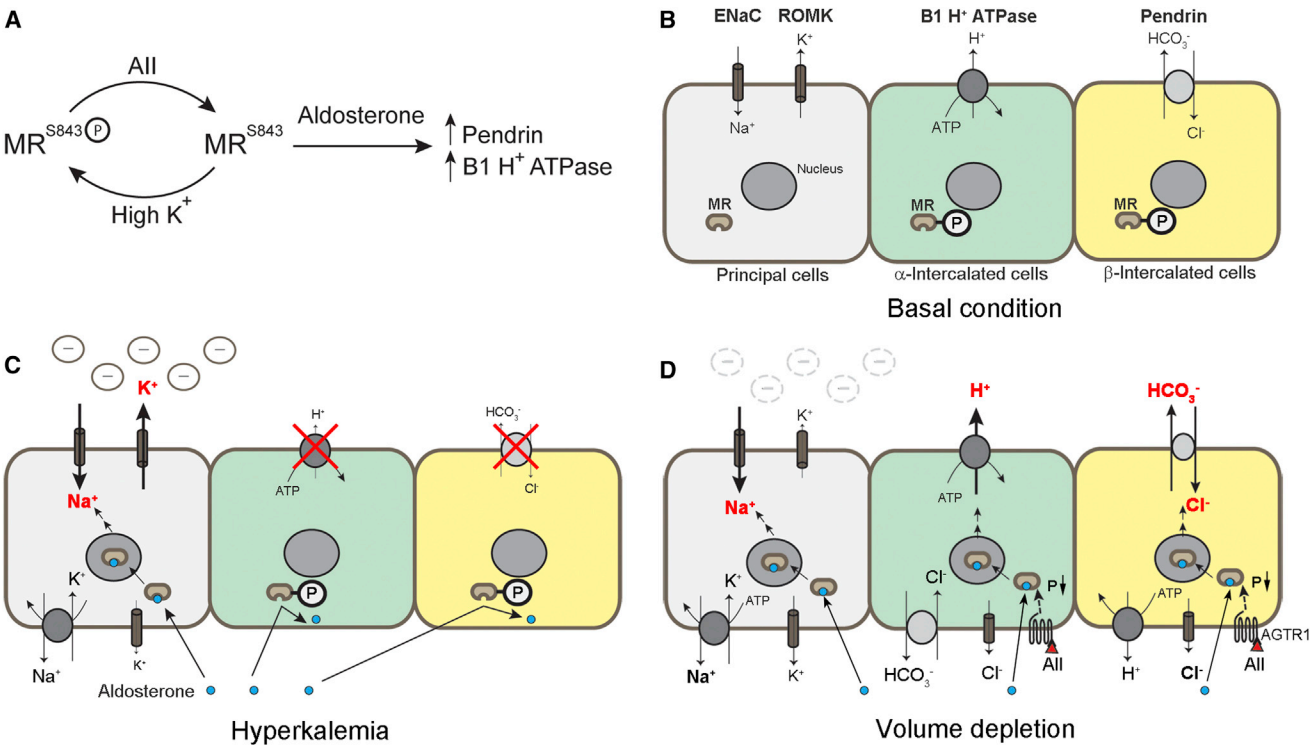

Figure 7. Physiologic Role of MR^{S843-P} in Response to Hyperkalemia and Volume Depletion

(A) Mechanism for MR-dependent regulation of pendrin and B1 H^+ ATPase in intercalated cells. High K^+ increases MR^{S843-P}, which prevents activation of MR by ligand. Dephosphorylation of MR^{S843-P} in response to AII signaling restores receptor competence and upregulation of pendrin and B1 H^+ ATPase in response to aldosterone.

(B) The major apical electrolyte flux mediators seen in the three major cells types of the CNT and CD of the distal nephron are shown. MR is present in all three; however, MR^{S843-P} (denoted "P") is only seen in intercalated cells.

(C) In hyperkalemia, aldosterone binds and activates MR in principal cells, but not in intercalated cells. This increases electrogenic Na^+ reabsorption via ENaC and provides the lumen-negative potential required for K^+ secretion.

(D) In volume depletion, in addition to MR signaling in principal cells, AII signaling reduces MR^{S843-P}, which results in MR signaling in intercalated cells. This results in Cl^- reabsorption via the combined activities of the apical H^+ ATPase and the apical Cl^-/HCO_3^- exchanger pendrin. Increased Cl^- reabsorption neutralizes the lumen-negative potential, preventing increased K^+ efflux. AGTR1, AII type 1 receptor. See also Figure S1.

K^+ secretion (Figure 7C). These changes are thus adaptive in promoting alternative responses to hypovolemia and hyperkalemia. These findings indicate the key role of AII signaling in switching the response to aldosterone from K^+ secretion to Na-Cl reabsorption and reveal how MR signaling can produce different responses to distinct physiologic conditions.

These conclusions are supported by prior work implicating β-intercalated cells in Cl^- reabsorption in the CD (Wall and Weinstein, 2013). Moreover, while *Slc12a3*$^{-/-}$ mice have modest salt wasting, adding *Pendrin* (*Slc26a4*) deficiency results in severe salt wasting, implicating pendrin in the normal adaptation to volume depletion (Soleimani et al., 2012). Our finding that MR^{S843-P} is dephosphorylated in *Slc12a3*$^{-/-}$ mice, resulting in upregulation of pendrin and H^+ ATPase, provides a mechanism for this compensation. We also infer that the metabolic alkalosis found in the double knockout mouse model can be explained by upregulation of apical H^+ ATPase without upregulation of pendrin (Figure 7A).

AII also increases NDCBE levels independent of MR. This suggests the potential to respond to combined volume depletion and hyperkalemia by induction of this intercalated cell Na-Cl reabsorption pathway while maintaining K^+ secretion due to the lumen-negative electrical gradient established by ENaC. The recognition of MR-dependent and independent pathways for salt reabsorption in the distal nephron raises the possibility for improved antihypertensive agents.

Biochemical details of the pathways that mediate and regulate MR^{S843-P} remain to be established. While dephosphorylation of S843 lies downstream of AII and WNK4 signaling, likely mediated by PP1, the intermediate steps are unknown. Specificity of phosphorylation at S843 could be achieved by selective expression of the responsible kinase in intercalated cells. It will be of interest to identify the kinase that directly phosphorylates S843 and the pathway linking hyperkalemia to increased S843 phosphorylation. Although knockdown of *WNK1* with siRNA reduced MR^{S843-P} levels by 32%, purified WNK1 did not phosphorylate MR^{S843-P} in vitro, suggesting that WNK1 does not directly phosphorylate MR^{S843} (Figures S7H and S7I). We predict that prevention of phosphorylation at 843 would produce hypertension and hyperkalemia.

Lastly, 11βHSD2, which metabolizes cortisol to the inactive metabolite cortisone (Funder et al., 1988), is thought to be absent

in some cell types that express MR (Kyossev et al., 1996; Nguyen Dinh Cat et al., 2010), posing the question of how MR is regulated in these cells. The finding of regulated ligand binding motivates further efforts to determine whether the same or related mechanisms may regulate MR activity in other tissues, and also whether posttranslational modification of other LBDs might play analogous roles to regulate ligand binding and activation.

EXPERIMENTAL PROCEDURES

Detailed methods are found in the Supplemental Experimental Procedures.

Identification of Phosphorylation Sites in MR

IP and LC-MS/MS were performed as described previously (Rinehart et al., 2009). Human MR with an N-terminal FLAG epitope (Shibata et al., 2008) was expressed in COS-7 cells and purified from cell lysates by FLAG-IP followed by SDS-PAGE. The resulting protein was digested with trypsin, and phosphopeptides were purified using TiO_2 affinity. Peptides were analyzed by mass spectrometry. The location of S843 in MR determined from the crystal structure of human MR bound to aldosterone (Protein Data Bank accession code 2AA2) (Bledsoe et al., 2005).

Analysis of MR Function

Transcriptional activity and ligand binding of WT and mutant MR were evaluated by luciferase reporter assay and receptor binding assay as described previously (Geller et al., 2000).

Western Blotting

Indicated cells and tissues were lysed and total protein, membrane, and nuclear and cytoplasmic fractions were prepared, subjected to western blotting, and probed with indicated antibodies.

To produce antibodies specific for MR phosphorylated at S843, the human MR peptide CKK-DLVFNEEKMHQS*AMYEL (*phospho-Ser), conjugated to CKK at the amino terminus, was coupled to keyhole limpet hemocyanin, and rabbits were immunized with the phosphopeptide (Covance Research Products). Pooled serum was depleted of nonspecific antibodies with the cognate nonphosphopeptide, and specific antibody was purified with the immunizing phosphopeptide. The antibody was used at a dilution of 1:100 for immunostaining and 1:3,000 for western blotting. In some experiments, samples were incubated with calf intestinal phosphatase at 37°C before western blotting. Other antibodies included antibodies to pendrin (1:10,000 for western blot and 1:400 for immunostaining; a gift from P. Aronson, Yale University); B1 H^+ ATPase (1:1,000 for Western blot and 1:100 for immunostaining, a gift of D. Brown, Massachusetts General Hospital); AE1 (1:100 for immunostaining, a gift of D. Biemesderfer, Yale University); MR (1:400 for western blotting and 1:50 for immunostaining, a gift of Dr. C.E. Gomez-Sanchez, University of Mississippi Health Center); AQP2 (1:250, Santa Cruz); WNK4 (1:100, prepared in our laboratory) (Wilson et al., 2001); NDCBE (1:1,000, Proteintech); FLAG (1:2,000), histone 1.4 (1:1,000), and α-tubulin (1:5,000) (all from Sigma); and 11βHSD2 (1:500, Millipore).

Immunofluorescence Microscopy

Cryosections from perfusion-fixed mouse kidneys or paraffin-embedded human kidney sections (use of normal human kidney from tissue removed at surgery for renal cancers was approved by Yale IRB) were incubated with indicated primary antibodies and secondary antibodies as described previously (Shibata et al., 2008).

Animal Studies

Mice were bred and maintained with approval by the Yale Institutional Animal Care and Use Committee. Mice studied included WT C57BL/6 mice, *Agtr1a*$^{-/-}$ mice (Ito et al., 1995) in the C57BL/6 background, *Slc12a3*$^{-/-}$ mice (Loffing et al., 2004) maintained on a mixed C57/BL6-129/SvJ background and WT littermates, *Wnk4*$^{-/-}$ mice in a C57/BL6-129/SvJ background (Castañeda-Bueno et al., 2012) and WT littermates, and mice transgenic for genomic segments harboring PHAII mutant *Wnk4* (Q562E; TgWNK4^{Q562E}) (Lalioti et al., 2006) in the C57BL/6 background. Dietary manipulations included high (8%) or low (0.03%) NaCl diet maintained for 12 days, and a high (5%) or normal (0.9%) K^+ diet for 7 days. For acid loading, drinking water contained 0.28 M NH_4Cl/1% sucrose for 7 days. Pharmacologic manipulation included subcutaneous infusion of 1 μg/kg/min AII or vehicle via osmotic minipump for 7 days (Gonzalez-Villalobos et al., 2008); the ARB losartan was administered orally at a dose of 30 mg/kg/day. The MRA spironolactone was given orally (0.2 g/kg chow). Aldosterone was administered subcutaneously at a dose of 50 μg/kg/day for 7 days (Leopold et al., 2007).

RNA Interference Studies and Kinase Assays

Previously characterized siRNA for *WNK1* (Rinehart et al., 2009) or control siRNA was introduced into HEK cells via transient transfection. For in vitro kinase assays, HA-tagged full-length rat WNK1 purified from COS-7 cells was incubated with purified FLAG-tagged MR in kinase buffer with ATP. MR phosphorylation was analyzed by western blotting and showed no increase in S843 phosphorylation.

Statistical Analysis

The data are summarized as means ± SEM. Unpaired t tests were used for comparisons between two groups. For multiple comparisons, statistical analysis was performed by ANOVA followed by Tukey post hoc tests. Correlation of changes in MR^{S843-P} and intercalated cell protein levels were tested by Pearson's correlation. $p < 0.05$ was considered significant.

SUPPLEMENTAL INFORMATION

Supplemental Information includes seven figures and Supplemental Experimental Procedures and can be found with this article at http://dx.doi.org/10.1016/j.cmet.2013.10.005.

ACKNOWLEDGMENTS

We thank Peter Aronson for helpful discussions and for providing pendrin antibody. We thank Mathieu Lemaire, Ute Scholl, and David Geller for helpful discussions. We thank Dennis Brown, Celso E. Gomez-Sanchez, and Daniel Biemesderfer for antibodies. We thank Hirotoshi Tanaka for MR plasmids. This work was supported in part by grants from the National Institutes of Health (P01-DK017433, P30-DK079310, UL1-RR024139, and K01-DK089006), the Leducq Transatlantic Network on Hypertension, and a fellowship grant from the Uehara Memorial Foundation. R.P.L. is an investigator of the Howard Hughes Medical Institute.

Received: August 1, 2012
Revised: July 29, 2013
Accepted: September 16, 2013
Published: November 5, 2013

REFERENCES

Ackermann, D., Gresko, N., Carrel, M., Loffing-Cueni, D., Habermehl, D., Gomez-Sanchez, C., Rossier, B.C., and Loffing, J. (2010). In vivo nuclear translocation of mineralocorticoid and glucocorticoid receptors in rat kidney: differential effect of corticosteroids along the distal tubule. Am. J. Physiol. Renal Physiol. *299*, F1473–F1485.

Alper, S.L., Natale, J., Gluck, S., Lodish, H.F., and Brown, D. (1989). Subtypes of intercalated cells in rat kidney collecting duct defined by antibodies against erythroid band 3 and renal vacuolar H+-ATPase. Proc. Natl. Acad. Sci. USA *86*, 5429–5433.

Arriza, J.L., Weinberger, C., Cerelli, G., Glaser, T.M., Handelin, B.L., Housman, D.E., and Evans, R.M. (1987). Cloning of human mineralocorticoid receptor complementary DNA: structural and functional kinship with the glucocorticoid receptor. Science *237*, 268–275.

Beauwens, R., Beaujean, V., Zizi, M., Rentmeesters, M., and Crabbé, J. (1986). Increased chloride permeability of amphibian epithelia treated with aldosterone. Pflugers Arch. *407*, 620–624.

Bledsoe, R.K., Madauss, K.P., Holt, J.A., Apolito, C.J., Lambert, M.H., Pearce, K.H., Stanley, T.B., Stewart, E.L., Trump, R.P., Willson, T.M., and Williams,

S.P. (2005). A ligand-mediated hydrogen bond network required for the activation of the mineralocorticoid receptor. J. Biol. Chem. *280*, 31283–31293.

Boyden, L.M., Choi, M., Choate, K.A., Nelson-Williams, C.J., Farhi, A., Toka, H.R., Tikhonova, I.R., Bjornson, R., Mane, S.M., Colussi, G., et al. (2012). Mutations in kelch-like 3 and cullin 3 cause hypertension and electrolyte abnormalities. Nature *482*, 98–102.

Castañeda-Bueno, M., Cervantes-Pérez, L.G., Vázquez, N., Uribe, N., Kantesaria, S., Morla, L., Bobadilla, N.A., Doucet, A., Alessi, D.R., and Gamba, G. (2012). Activation of the renal Na+:Cl- cotransporter by angiotensin II is a WNK4-dependent process. Proc. Natl. Acad. Sci. USA *109*, 7929–7934.

Chen, D., Pace, P.E., Coombes, R.C., and Ali, S. (1999). Phosphorylation of human estrogen receptor alpha by protein kinase A regulates dimerization. Mol. Cell. Biol. *19*, 1002–1015.

Choi, J.H., Banks, A.S., Estall, J.L., Kajimura, S., Boström, P., Laznik, D., Ruas, J.L., Chalmers, M.J., Kamenecka, T.M., Blüher, M., et al. (2010). Anti-diabetic drugs inhibit obesity-linked phosphorylation of PPARgamma by Cdk5. Nature *466*, 451–456.

Faresse, N., Vitagliano, J.J., and Staub, O. (2012). Differential ubiquitylation of the mineralocorticoid receptor is regulated by phosphorylation. FASEB J. *26*, 4373–4382.

Finberg, K.E., Wagner, C.A., Stehberger, P.A., Geibel, J.P., and Lifton, R.P. (2003). Molecular cloning and characterization of Atp6v1b1, the murine vacuolar H+ -ATPase B1-subunit. Gene *318*, 25–34.

Frische, S., Kwon, T.H., Frøkiaer, J., Madsen, K.M., and Nielsen, S. (2003). Regulated expression of pendrin in rat kidney in response to chronic NH4Cl or NaHCO3 loading. Am. J. Physiol. Renal Physiol. *284*, F584–F593.

Funder, J.W., Pearce, P.T., Smith, R., and Smith, A.I. (1988). Mineralocorticoid action: target tissue specificity is enzyme, not receptor, mediated. Science *242*, 583–585.

Geller, D.S., Rodriguez-Soriano, J., Vallo Boado, A., Schifter, S., Bayer, M., Chang, S.S., and Lifton, R.P. (1998). Mutations in the mineralocorticoid receptor gene cause autosomal dominant pseudohypoaldosteronism type I. Nat. Genet. *19*, 279–281.

Geller, D.S., Farhi, A., Pinkerton, N., Fradley, M., Moritz, M., Spitzer, A., Meinke, G., Tsai, F.T., Sigler, P.B., and Lifton, R.P. (2000). Activating mineralocorticoid receptor mutation in hypertension exacerbated by pregnancy. Science *289*, 119–123.

Glass, C.K., and Rosenfeld, M.G. (2000). The coregulator exchange in transcriptional functions of nuclear receptors. Genes Dev. *14*, 121–141.

Gomez-Sanchez, C.E., de Rodriguez, A.F., Romero, D.G., Estess, J., Warden, M.P., Gomez-Sanchez, M.T., and Gomez-Sanchez, E.P. (2006). Development of a panel of monoclonal antibodies against the mineralocorticoid receptor. Endocrinology *147*, 1343–1348.

Gonzalez-Villalobos, R.A., Seth, D.M., Satou, R., Horton, H., Ohashi, N., Miyata, K., Katsurada, A., Tran, D.V., Kobori, H., and Navar, L.G. (2008). Intrarenal angiotensin II and angiotensinogen augmentation in chronic angiotensin II-infused mice. Am. J. Physiol. Renal Physiol. *295*, F772–F779.

Ito, M., Oliverio, M.I., Mannon, P.J., Best, C.F., Maeda, N., Smithies, O., and Coffman, T.M. (1995). Regulation of blood pressure by the type 1A angiotensin II receptor gene. Proc. Natl. Acad. Sci. USA *92*, 3521–3525.

Kahle, K.T., Wilson, F.H., Leng, Q., Lalioti, M.D., O'Connell, A.D., Dong, K., Rapson, A.K., MacGregor, G.G., Giebisch, G., Hebert, S.C., and Lifton, R.P. (2003). WNK4 regulates the balance between renal NaCl reabsorption and K+ secretion. Nat. Genet. *35*, 372–376.

Kahle, K.T., Ring, A.M., and Lifton, R.P. (2008). Molecular physiology of the WNK kinases. Annu. Rev. Physiol. *70*, 329–355.

Kino, T., Jaffe, H., Amin, N.D., Chakrabarti, M., Zheng, Y.L., Chrousos, G.P., and Pant, H.C. (2010). Cyclin-dependent kinase 5 modulates the transcriptional activity of the mineralocorticoid receptor and regulates expression of brain-derived neurotrophic factor. Mol. Endocrinol. *24*, 941–952.

Kyossev, Z., Walker, P.D., and Reeves, W.B. (1996). Immunolocalization of NAD-dependent 11 beta-hydroxysteroid dehydrogenase in human kidney and colon. Kidney Int. *49*, 271–281.

Lalioti, M.D., Zhang, J., Volkman, H.M., Kahle, K.T., Hoffmann, K.E., Toka, H.R., Nelson-Williams, C., Ellison, D.H., Flavell, R., Booth, C.J., et al. (2006). Wnk4 controls blood pressure and potassium homeostasis via regulation of mass and activity of the distal convoluted tubule. Nat. Genet. *38*, 1124–1132.

Leopold, J.A., Dam, A., Maron, B.A., Scribner, A.W., Liao, R., Handy, D.E., Stanton, R.C., Pitt, B., and Loscalzo, J. (2007). Aldosterone impairs vascular reactivity by decreasing glucose-6-phosphate dehydrogenase activity. Nat. Med. *13*, 189–197.

Leviel, F., Hübner, C.A., Houillier, P., Morla, L., El Moghrabi, S., Brideau, G., Hassan, H., Parker, M.D., Kurth, I., Kougioumtzes, A., et al. (2010). The Na+-dependent chloride-bicarbonate exchanger SLC4A8 mediates an electroneutral Na+ reabsorption process in the renal cortical collecting ducts of mice. J. Clin. Invest. *120*, 1627–1635.

Lin, H.K., Wang, L., Hu, Y.C., Altuwaijri, S., and Chang, C. (2002). Phosphorylation-dependent ubiquitylation and degradation of androgen receptor by Akt require Mdm2 E3 ligase. EMBO J. *21*, 4037–4048.

Lin, D.H., Yue, P., Rinehart, J., Sun, P., Wang, Z., Lifton, R., and Wang, W.H. (2012). Protein phosphatase 1 modulates the inhibitory effect of With-no-Lysine kinase 4 on ROMK channels. Am. J. Physiol. Renal Physiol. *303*, F110–F119.

Loffing, J., Vallon, V., Loffing-Cueni, D., Aregger, F., Richter, K., Pietri, L., Bloch-Faure, M., Hoenderop, J.G., Shull, G.E., Meneton, P., and Kaissling, B. (2004). Altered renal distal tubule structure and renal Na(+) and Ca(2+) handling in a mouse model for Gitelman's syndrome. J. Am. Soc. Nephrol. *15*, 2276–2288.

Mangelsdorf, D.J., Thummel, C., Beato, M., Herrlich, P., Schütz, G., Umesono, K., Blumberg, B., Kastner, P., Mark, M., Chambon, P., and Evans, R.M. (1995). The nuclear receptor superfamily: the second decade. Cell *83*, 835–839.

McKenna, N.J., and O'Malley, B.W. (2002). Combinatorial control of gene expression by nuclear receptors and coregulators. Cell *108*, 465–474.

Nguyen Dinh Cat, A., Griol-Charhbili, V., Loufrani, L., Labat, C., Benjamin, L., Farman, N., Lacolley, P., Henrion, D., and Jaisser, F. (2010). The endothelial mineralocorticoid receptor regulates vasoconstrictor tone and blood pressure. FASEB J. *24*, 2454–2463.

Ortlund, E.A., Bridgham, J.T., Redinbo, M.R., and Thornton, J.W. (2007). Crystal structure of an ancient protein: evolution by conformational epistasis. Science *317*, 1544–1548.

Pech, V., Zheng, W., Pham, T.D., Verlander, J.W., and Wall, S.M. (2008). Angiotensin II activates H+-ATPase in type A intercalated cells. J. Am. Soc. Nephrol. *19*, 84–91.

Pitt, B., Reichek, N., Willenbrock, R., Zannad, F., Phillips, R.A., Roniker, B., Kleiman, J., Krause, S., Burns, D., and Williams, G.H. (2003). Effects of eplerenone, enalapril, and eplerenone/enalapril in patients with essential hypertension and left ventricular hypertrophy: the 4E-left ventricular hypertrophy study. Circulation *108*, 1831–1838.

Pratt, W.B. (1997). The role of the hsp90-based chaperone system in signal transduction by nuclear receptors and receptors signaling via MAP kinase. Annu. Rev. Pharmacol. Toxicol. *37*, 297–326.

Reilly, R.F., and Ellison, D.H. (2000). Mammalian distal tubule: physiology, pathophysiology, and molecular anatomy. Physiol. Rev. *80*, 277–313.

Rinehart, J., Maksimova, Y.D., Tanis, J.E., Stone, K.L., Hodson, C.A., Zhang, J., Risinger, M., Pan, W., Wu, D., Colangelo, C.M., et al. (2009). Sites of regulated phosphorylation that control K-Cl cotransporter activity. Cell *138*, 525–536.

Rochette-Egly, C., Adam, S., Rossignol, M., Egly, J.M., and Chambon, P. (1997). Stimulation of RAR alpha activation function AF-1 through binding to the general transcription factor TFIIH and phosphorylation by CDK7. Cell *90*, 97–107.

Rothenberger, F., Velic, A., Stehberger, P.A., Kovacikova, J., and Wagner, C.A. (2007). Angiotensin II stimulates vacuolar H+ -ATPase activity in renal acid-secretory intercalated cells from the outer medullary collecting duct. J. Am. Soc. Nephrol. *18*, 2085–2093.

San-Cristobal, P., Pacheco-Alvarez, D., Richardson, C., Ring, A.M., Vazquez, N., Rafiqi, F.H., Chari, D., Kahle, K.T., Leng, Q., Bobadilla, N.A., et al. (2009).

Angiotensin II signaling increases activity of the renal Na-Cl cotransporter through a WNK4-SPAK-dependent pathway. Proc. Natl. Acad. Sci. USA *106*, 4384–4389.

Shao, D., Rangwala, S.M., Bailey, S.T., Krakow, S.L., Reginato, M.J., and Lazar, M.A. (1998). Interdomain communication regulating ligand binding by PPAR-gamma. Nature *396*, 377–380.

Shibata, S., Nagase, M., Yoshida, S., Kawarazaki, W., Kurihara, H., Tanaka, H., Miyoshi, J., Takai, Y., and Fujita, T. (2008). Modification of mineralocorticoid receptor function by Rac1 GTPase: implication in proteinuric kidney disease. Nat. Med. *14*, 1370–1376.

Shibata, S., Zhang, J., Puthumana, J., Stone, K.L., and Lifton, R.P. (2013). Kelch-like 3 and Cullin 3 regulate electrolyte homeostasis via ubiquitination and degradation of WNK4. Proc. Natl. Acad. Sci. USA *110*, 7838–7843.

Soleimani, M., Barone, S., Xu, J., Shull, G.E., Siddiqui, F., Zahedi, K., and Amlal, H. (2012). Double knockout of pendrin and Na-Cl cotransporter (NCC) causes severe salt wasting, volume depletion, and renal failure. Proc. Natl. Acad. Sci. USA *109*, 13368–13373.

Spät, A., and Hunyady, L. (2004). Control of aldosterone secretion: a model for convergence in cellular signaling pathways. Physiol. Rev. *84*, 489–539.

Wakabayashi, M., Mori, T., Isobe, K., Sohara, E., Susa, K., Araki, Y., Chiga, M., Kikuchi, E., Nomura, N., Mori, Y., et al. (2013). Impaired KLHL3-mediated ubiquitination of WNK4 causes human hypertension. Cell Rep. *3*, 858–868.

Wall, S.M., and Pech, V. (2008). The interaction of pendrin and the epithelial sodium channel in blood pressure regulation. Curr. Opin. Nephrol. Hypertens. *17*, 18–24.

Wall, S.M., and Weinstein, A.M. (2013). Cortical distal nephron Cl- transport in volume homeostasis and blood pressure regulation. Am. J. Physiol. Renal Physiol. *305*, F427–F438.

Wilson, F.H., Disse-Nicodème, S., Choate, K.A., Ishikawa, K., Nelson-Williams, C., Desitter, I., Gunel, M., Milford, D.V., Lipkin, G.W., Achard, J.M., et al. (2001). Human hypertension caused by mutations in WNK kinases. Science *293*, 1107–1112.

Wilson, F.H., Kahle, K.T., Sabath, E., Lalioti, M.D., Rapson, A.K., Hoover, R.S., Hebert, S.C., Gamba, G., and Lifton, R.P. (2003). Molecular pathogenesis of inherited hypertension with hyperkalemia: the Na-Cl cotransporter is inhibited by wild-type but not mutant WNK4. Proc. Natl. Acad. Sci. USA *100*, 680–684.

Yang, C.L., Angell, J., Mitchell, R., and Ellison, D.H. (2003). WNK kinases regulate thiazide-sensitive Na-Cl cotransport. J. Clin. Invest. *111*, 1039–1045.

Yin, L., Wang, J., Klein, P.S., and Lazar, M.A. (2006). Nuclear receptor Rev-erbalpha is a critical lithium-sensitive component of the circadian clock. Science *311*, 1002–1005.